



Characterization of topological phase of superlattices in superconducting circuits

Jianfei Chen(陈健菲), Chaohua Wu(吴超华), Jingtao Fan(樊景涛), and Gang Chen(陈刚)

Citation: Chin. Phys. B, 2022, 31 (8): 088501. DOI: 10.1088/1674-1056/ac5612

Journal homepage: <http://cpb.iphy.ac.cn>; <http://iopscience.iop.org/cpb>

What follows is a list of articles you may be interested in

Shortcut-based quantum gates on superconducting qubits in circuit QED

Zheng-Yin Zhao(赵正印), Run-Ying Yan(闫润璘), and Zhi-Bo Feng(冯志波)

Chin. Phys. B, 2021, 30 (8): 088501. DOI: 10.1088/1674-1056/abea96

Characteristics and mechanisms of subthreshold voltage hysteresis in 4H-SiC MOSFETs

Xi-Ming Chen(陈喜明), Bang-Bing Shi(石帮兵), Xuan Li(李轩), Huai-Yun Fan(范怀云), Chen-Zhan Li(李诚瞻),

Xiao-Chuan Deng(邓小川), Hai-Hui Luo(罗海辉), Yu-Dong Wu(吴煜东), and Bo Zhang(张波)

Chin. Phys. B, 2021, 30 (4): 048504. DOI: 10.1088/1674-1056/abd391

Negative gate bias stress effects on conduction and low frequency noise characteristics in p-type poly-Si thin-film transistors

Chao-Yang Han(韩朝阳), Yuan Liu(刘远), Yu-Rong Liu(刘玉荣), Ya-Yi Chen(陈雅怡), Li Wang(王黎), Rong-Sheng Chen(陈荣盛)

Chin. Phys. B, 2019, 28 (8): 088502. DOI: 10.1088/1674-1056/28/8/088502

Influence of white light illumination on the performance of a-IGZO thin film transistor under positive gate-bias stress

Tang Lan-Feng, Yu Guang, Lu Hai, Wu Chen-Fei, Qian Hui-Min, Zhou Dong, Zhang Rong, Zheng You-Dou, Huang Xiao-Ming

Chin. Phys. B, 2015, 24 (8): 088504. DOI: 10.1088/1674-1056/24/8/088504

Low frequency noise and radiation response in the partially depleted SOI MOSFETs with ion implanted buried oxide

Liu Yuan, Chen Hai-Bo, Liu Yu-Rong, Wang Xin, En Yun-Fei, Li Bin, Lu Yu-Dong

Chin. Phys. B, 2015, 24 (8): 088503. DOI: 10.1088/1674-1056/24/8/088503

CPB

Chinese Physics B

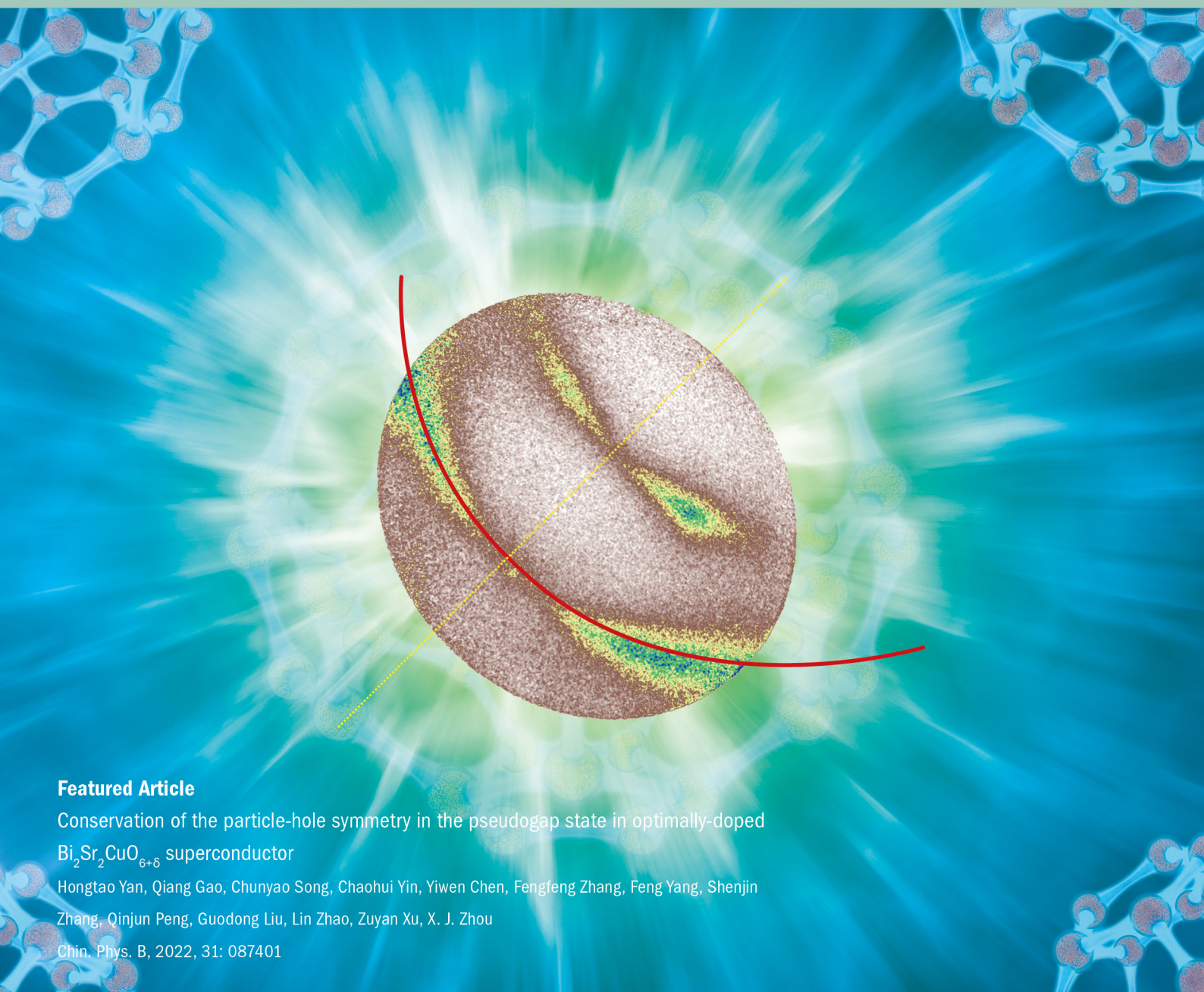
Volume 31 August 2022 Number 8

TOPICAL REVIEW

• Celebrating 30 Years of *Chinese Physics B*

A series Journal of the Chinese Physical Society Distributed by IOP Publishing

iopscience.org/cpb | cpb.iphy.ac.cn



Featured Article

Conservation of the particle-hole symmetry in the pseudogap state in optimally-doped $\text{Bi}_2\text{Sr}_2\text{CuO}_{6+\delta}$ superconductor

Hongtao Yan, Qiang Gao, Chunyao Song, Chaohui Yin, Yiwen Chen, Fengfeng Zhang, Feng Yang, Shenjin

Zhang, Qinjun Peng, Guodong Liu, Lin Zhao, Zuyan Xu, X. J. Zhou

Chin. Phys. B, 2022, 31: 087401

Chinese Physics B (中国物理B)

First published in 1992. Published monthly in hard copy by the Chinese Physical Society and online by IOP Publishing, Temple Circus, Temple Way, Bristol BS1 6HG, UK

Institutional subscription information: 2022 volume

For all countries, except the United States, Canada and Central and South America, the subscription rate per annual volume is UK£1397 (electronic only) or UK£1523 (print + electronic).

Delivery is by air-speeded mail from the United Kingdom.

Orders to:

Journals Subscription Fulfilment, IOP Publishing, Temple Circus, Temple Way, Bristol BS1 6HG, UK

For the United States, Canada and Central and South America, the subscription rate per annual volume is US\$2780 (electronic only) or US\$3025 (print + electronic). Delivery is by transatlantic airfreight and onward mailing.

Orders to: IOP Publishing, P. O. Box 320, Congers, NY 10920-0320, USA

© 2022 Chinese Physical Society and IOP Publishing Ltd

All rights reserved. No part of this publication may be reproduced, stored in a retrieval system, or transmitted in any form or by any means, electronic, mechanical, photocopying, recording or otherwise, without the prior written permission of the copyright owner.

Editorial Office: Institute of Physics, Chinese Academy of Sciences, P. O. Box 603, Beijing 100190, China

Tel: (86-10) 82649026 or 82649519, Fax: (86-10) 82649027, E-mail: cpb@aphy.iphy.ac.cn

主管单位: 中国科学院

国际统一刊号: ISSN 1674-1056

主办单位: 中国物理学会和中国科学院物理研究所

国内统一刊号: CN 11-5639/O4

编辑: Chinese Physics B 编辑部

编辑部地址: 北京 中关村 中国科学院物理研究所内

出版: 中国物理学会

通信地址: 100190 北京 603 信箱

出版日期: 2022年8月

电话: (010) 82649026, 82649519

印刷装订: 北京科信印刷有限公司

传真: (010) 82649027

国内发行: Chinese Physics B 编辑部

“Chinese Physics B”网址:

国外发行: IOP Publishing Ltd

<http://cpb.iphy.ac.cn>

发行范围: 公开发行

<http://iopscience.iop.org/journal/1674-1056>

Advisory Board

Chen Jia-Er(陈佳洱), T. D. Lee(李政道), Samuel C. C. Ting(丁肇中), C. N. Yang(杨振宁), Yang Fu-Jia(杨福家), Wang Nai-Yan(王乃彦), Zhao Zhong-Xian(赵忠贤), Yang Guo-Zhen(杨国桢)

Editorial Board

Editor-in-Chief

Gao Hong-Jun(高鸿钧)

Chinese Academy of Sciences, China

Associate Editors

Chen Xian-Hui(陈仙辉)

University of Science and Technology of China, China

Fan Heng(范桁)

Institute of Physics, Chinese Academy of Sciences, China

Gao Yuan-Ning(高原宁)

Peking University, China

Li Jian-Xin(李建新)

Nanjing University, China

Li Ru-Xin(李儒新)

Shanghai Tech University, China

Ma Yan-Ming(马琰铭)

Jilin University, China

Ouyang Zhong-Can(欧阳钟灿) Institute of Theoretical Physics, Chinese Academy of Sciences, China
Shen Bao-Gen(沈保根) Institute of Physics, Chinese Academy of Sciences, China
Wang Wei-Hua(汪卫华) Institute of Physics, Chinese Academy of Sciences, China
Wang Zi-Qiang(汪自强) Boston College USA
Wang Ning(王宁) The Hong Kong University of Science & Technology, China
Xiong Qi-Hua(熊启华) Tsinghua University, China
Yao Wang(姚望) The University of Hong Kong, China
Zhang Jie(张杰) Chinese Physical Society, China
Zhang Yuan-Bo(张远波) Fudan University, China

Editorial Board

Chen Chong-Lin(陈充林) University of Texas at San Antonio, USA
Chen Wei(陈伟) National University of Singapore, Singapore
Chen Xiao-Song(陈晓松) Beijing Normal University, China
Chen Yu-Ao(陈宇翱) University of Science and Technology of China, China
Cheng Jian-Chun(程建春) Nanjing University, China
Cheng Meng(程蒙) Yale University, USA
Cui Xiao-Dong(崔晓冬) The University of Hong Kong, China
Dai Qing(戴庆) National Center for Nanoscience and Technology, China
Ding Da-Jun(丁大军) Jilin University, China
Fang Zhong(方忠) Institute of Physics, Chinese Academy of Sciences, China
Feng Shi-Ping(冯世平) Beijing Normal University, China
Feng Xin-Liang(冯新亮) Dresden University of Technology, Germany
Gao Wei-Bo(高炜博) Nanyang Technological University, Singapore
Gong Xin-Gao(龚新高) Fudan University, China
Gu Chang-Zhi(顾长志) Institute of Physics, Chinese Academy of Sciences, China
Guo Hong(郭鸿) McGill University, Canada
Hu Xiao(胡晓) National Institute for Materials Science, Japan
Huang Xue-Jie(黄学杰) Institute of Physics, Chinese Academy of Sciences, China
Ji Wei(季威) Renmin University of China, China
Jia Jin-Feng(贾金锋) Shanghai Jiao Tong University, China
Jiang Ying(江颖) Peking University, China
Leong Chuan Kwek National University of Singapore, Singapore
Lei Dangyuan(雷党愿) City University of Hong Kong, China
Li Bao-Wen(李保文) University of Colorado Boulder, USA
Li Jian-Qi(李建奇) Institute of Physics, Chinese Academy of Sciences, China
Li Xiao-Guang(李晓光) University of Science and Technology of China, China
Liu Bing-Bing(刘冰冰) Jilin University, China
Liu Chao-Xing(刘朝星) Pennsylvania State University, USA
Liu Xiang-Yang(刘向阳) Xiamen University, China
Liu Yi-Chun(刘益春) Northeast Normal University, China
Liu Zheng(刘政) Nanyang Technological University, Singapore
Long Gui-Lu(龙桂鲁) Tsinghua University, China
Lu Zheng-Tian(卢征天) University of Science and Technology of China, China
Lu Dong-Hui(路东辉) Stanford Synchrotron Radiation Lightsource, SLAC National Accelerator Laboratory, USA
Lu Wei(陆卫) Shanghai Institute of Technical Physics, Chinese Academy of Sciences, China
Luo Hong-Gang(罗洪刚) Lanzhou University, China
Lu Guang-Hong(吕广宏) Beihang University, China
Lu Li(吕力) Institute of Physics, Chinese Academy of Sciences, China

Ma Xu-Cun(马旭村)	Tsinghua University, China
Ma Yu-Gang(马余刚)	Fudan University, China
Ni Pei-Gen(倪培根)	National Natural Science Foundation of China, China
Niu Qian(牛谦)	University of Texas, USA
Ouyang Qi(欧阳颀)	Peking University, China
Pan Yi(潘毅)	Xi'an Jiaotong University, China
Shen De-Zhen(申德振)	Changchun Institute of Optics, Fine Mechanics and Physics, Chinese Academy of Sciences, China
Shen Ze-Xiang(申泽骧)	Nanyang Technological University, Singapore
Shen Jian(沈健)	Fudan University, China
Si Qi-Miao(斯其苗)	Rice University, USA
Sun Chang-Pu(孙昌璞)	Beijing Computational Science Research Center, China
Sun Xiao Wei(孙小卫)	Southern University of Science and Technology, China
Tian Yong-Jun(田永君)	Yanshan University, China
Tong Li-Min(童利民)	Zhejiang University, China
John S. Tse	University of Saskatchewan, Canada
Wan Bao-Nian(万宝年)	Institute of Plasma Physics, Chinese Academy of Sciences, China
Wang Bo-Gen(王伯根)	Nanjing University, China
Wang Kai-You(王开友)	Institute of Semiconductors, Chinese Academy of Sciences, China
Wang Wei(王炜)	Nanjing University, China
Wang Ya-Yu(王亚愚)	Tsinghua University, China
Wang Yu-Peng(王玉鹏)	Institute of Physics, Chinese Academy of Sciences, China
Wei Su-Huai(魏苏淮)	Beijing Computational Science Research Center, China
Wen Wei-Jia(温维佳)	The Hong Kong University of Science & Technology, China
Wen Hai-Hu(闻海虎)	Nanjing University, China
Wu Nan-Jian(吴南健)	Institute of Semiconductors, Chinese Academy of Sciences, China
Xiang Tao(向涛)	Institute of Physics, Chinese Academy of Sciences, China
Xiao Di(肖迪)	Carnegie Mellon University, USA
Xie Xin-Cheng(谢心澄)	Peking University, China
Xu Hong-Xing(徐红星)	Wuhan University, China
Xu Zhi-Chuan(徐志川)	Nanyang Technological University, Singapore
Xu Xiao-Dong(许晓栋)	University of Washington, USA
Yang Guo-Wei(杨国伟)	Sun Yat-Sen University, China
Yang Lan(杨兰)	Washington University in St. Louis, USA
Ye Jun(叶军)	University of Colorado, USA
Zhang Fu-Chun(张富春)	University of Chinese Academy of Sciences, China
Zhang Hong(张红)	Sichuan University, China
Zhang Yong(张勇)	The University of North Carolina at Charlotte, USA
Zhang Zhen-Yu(张振宇)	University of Science and Technology of China, China
Zhao Hong-Wei(赵红卫)	Institute of Modern Physics, Chinese Academy of Sciences, China
Zhao Hui(赵辉)	The University of Kansas, USA
Zhao Wei-Juan(赵维娟)	Zhengzhou University, China
Zheng Zhi-Gang(郑志刚)	Huaqiao University, China
Zhou Wu(周武)	University of Chinese Academy of Sciences, China
Zhou Xin(周昕)	University of Chinese Academy of Sciences, China
Zhou Xin(周欣)	Wuhan Institute of Physics and Mathematics, Chinese Academy of Sciences, China
Zhou Xing-Jiang(周兴江)	Institute of Physics, Chinese Academy of Sciences, China
Zhu Bang-Fen(朱邦芬)	Tsinghua University, China

Editorial Staff

Wang Jiu-Li(王久丽) (Editorial Director) Cai Jian-Wei(蔡建伟) Zhai Zhen(翟振)

Characterization of topological phase of superlattices in superconducting circuits

Jianfei Chen(陈健菲)^{1,2}, Chaohua Wu(吴超华)^{1,2,†}, Jingtao Fan(樊景涛)^{1,2}, and Gang Chen(陈刚)^{1,2,3}

¹State Key Laboratory of Quantum Optics and Quantum Optics Devices, Institute of Laser Spectroscopy, Shanxi University, Taiyuan 030006, China

²Collaborative Innovation Center of Extreme Optics, Shanxi University, Taiyuan 030006, China

³Collaborative Innovation Center of Light Manipulations and Applications, Shandong Normal University, Jinan 250358, China

(Received 30 October 2021; revised manuscript received 14 February 2022; accepted manuscript online 17 February 2022)

The recent experimental observation of topological magnon insulator states in a superconducting circuit chain marks a breakthrough for topological physics with qubits, in which a dimerized qubit chain has been realized. Here, we extend such a dimer lattice to superlattice with arbitrary number of qubits in each unit cell in superconducting circuits, which exhibits rich topological properties. Specifically, by considering a quadrimeric superlattice, we show that the topological invariant (winding number) can be effectively characterized by the dynamics of the single-excitation quantum state through time-dependent quantities. Moreover, we explore the appearance and detection of the topological protected edge states in such a multiband qubit system. Finally, we also demonstrate the stable Bloch-like-oscillation of multiple interface states induced by the interference of them. Our proposal can be readily realized in experiment and may pave the way towards the investigation of topological quantum phases and topologically protected quantum information processing.

Keywords: superconducting circuits, topological phase transition, edge state, interface state

PACS: 85.25.-j, 03.67.Ac

DOI: 10.1088/1674-1056/ac5612

1. Introduction

As one of the leading quantum platforms for implementing scalable quantum computation,^[1–3] superconducting circuits have achieved great experimental progress in the past few years. In particular, due to the site-specific control and read-out techniques, as well as the flexible and engineerable system designs,^[4–6] a superconducting circuit system has emerged as a rich platform for quantum simulation.^[7–10] By performing analog quantum simulations, a wide range of many-body physics has been employed in such simulators, such as the Bose–Hubbard model,^[11–13] many-body localization,^[14–18] quantum walks,^[19–21] and dynamical phase transitions.^[22] Moreover, due to the flexibility and diversity of superconducting quantum circuits system, it is also an excellent platform to realize exotic topological phases of matter and to probe and explore topologically protected effects, including the detection of topological invariant,^[23] topological state transfer,^[24,25] and higher-order topological phases.^[26,27]

In a recent experiment,^[28] topological magnon insulator states have been observed in a one-dimensional (1D) superconducting qubit chain with a tunable dimerized spin chain, which is analogue to the Su–Schrieffer–Heeger (SSH) model with two bands. Actually, various extended SSH models have been proposed to study novel topological physics by considering some other modulation terms, such as long range hoppings,^[29] periodically driving,^[30–32] and non-Hermitian modulation.^[33–36] Recently, 1D superlattices with multiple sites (> 2) in each unit cell have garnered much interest.^[37–40]

Such multiband systems show richer topological features than two-band models, such as the ability to tune the number of topological edge states by controlling the couplings, which allow one flexible control over the topological states in a new domain. Moreover, the superlattices with even sites in each unit cell preserve the chiral symmetry, and the topological phases can be characterized by the winding number.

In this work, we present an experimental feasible scheme to achieve the simulation of topological superlattice in a superconducting qubit chain with tunable coupling strengths. Such one-dimensional superlattices possess multiple topologically nontrivial dispersion bands and tunable edge states. Specifically, by considering a quadrimeric superlattice (SSH₄ model), we show that the topological invariant (winding number) can be effectively characterized by the dynamics of the single-excitation quantum state through an extended mean chiral displacement. Moreover, we explore the appearance and detection of the topological protected edge states in our qubit system. Finally, we also demonstrate the Bloch-oscillation-like dynamics induced by the interference of topological interface states with different propagation constants.

This article is organized as follows. Section 2 gives the feasible method to achieve one-dimensional superlattice in superconducting circuits. Section 3 demonstrates the measurement of topological winding number for quadrimeric lattice. Section 4 explores the existence and detection of topological edge states. Section 5 shows the dynamics of interface state propagation.

[†]Corresponding author. E-mail: sxwuchua@163.com

2. Model and Hamiltonian

Based on the recent experiment,^[28] we consider a one-dimensional spin chain consisting of N capacitively coupled qubits as shown in Fig. 1(a). The Hamiltonian of the system can be expressed as

$$\mathcal{H} = \sum_{j=0}^{N-1} \frac{\omega_j}{2} \sigma_j^+ \sigma_j^- + \sum_{j=1}^{N-1} g_j \left(\sigma_{j-1}^+ + \sigma_{j-1}^- \right) \left(\sigma_j^+ + \sigma_j^- \right), \quad (1)$$

where σ_j^+ (σ_j^-) is the raising (lowering) operator of the j th qubit Q_j with transition frequency ω_j . The parameter g_j denotes the coupling strength between qubits Q_{j-1} and Q_j . In general, the coupling strengths are not adjustable. To achieve fully tunable coupling strengths, one can apply an ac magnetic flux to periodically modulate the qubit frequencies,^[41,42]

$$\omega_j = \bar{\omega}_j + \varepsilon_j \sin(v_j t + \varphi_j), \quad (2)$$

where $\bar{\omega}_j$ is the mean operating frequency, ε_j , v_j , and φ_j are the modulation amplitude, frequency, and phase respectively. By defining a rotating frame $U = U_1 \times U_2$ with

$$U_1 = \exp \left[-i \left(\sum_{j=0}^{N-1} \frac{\bar{\omega}_j}{2} \sigma_j^z \right) t \right], \quad (3)$$

$$U_2 = \exp \left[i \sum_{j=0}^{N-1} \sigma_j^z \frac{\alpha_j}{2} \cos(v_j t + \varphi_j) \right], \quad (4)$$

where $\alpha_j = \varepsilon_j/v_j$, we can obtain the transformed Hamiltonian

$$\begin{aligned} \mathcal{H}_1 &= i \frac{dU^\dagger}{dt} U + U^\dagger H U \\ &= \sum_{j=1}^{N-1} g_j \left\{ \sigma_{j-1}^+ \sigma_j^- e^{i\Delta_j t} \exp[-i\alpha_{j-1} \cos(v_{j-1}t + \varphi_{j-1})] \right. \\ &\quad \left. \exp[i\alpha_j \cos(v_j t + \varphi_j)] + \text{H.c.} \right\}, \end{aligned} \quad (5)$$

where $\Delta_j = \bar{\omega}_j - \bar{\omega}_{j-1}$. We consider $\Delta_j = v_j(-v_j)$ for odd (even) j .^[41] Then, using the Jacobi–Anger identity

$$\exp[i\alpha \cos(vt + \varphi)] = \sum_{l=-\infty}^{\infty} i^l \mathcal{J}_l(\alpha) e^{il(vt + \varphi)}, \quad (6)$$

with $\mathcal{J}_l(\alpha)$ being the l th Bessel function of the first kind, and applying the rotating-wave approximation by neglecting the high-order oscillation terms, the effective Hamiltonian becomes

$$\mathcal{H}_{\text{eff}} = \sum_{j=1}^{N-1} g'_j \sigma_{j-1}^+ \sigma_j^- + \text{H.c.}, \quad (7)$$

with the effective coupling strength

$$g'_j = g_j \mathcal{J}_1(\alpha_j) \mathcal{J}_0(\alpha_{j-1}) e^{\pm i(\varphi_j \pm \pi/2)}, \quad (8)$$

where \pm denotes j being odd and even in g'_j , respectively. From Eq. (8), it is clear that the coupling strength g'_j can

be conveniently tuned independently by changing $\alpha_j = \varepsilon_j/v_j$. Moreover, there is a phase factor in each coupling which is derived from the driving phase φ_j . Such a superconducting qubit chain with tunable couplings can be used to study quantum state transfer,^[43] quantum gate,^[44] and gauge potentials.^[45] Moreover, we can realize generalized superlattice in addition to the simple SSH model in such a qubit chain with fully tunable couplings.

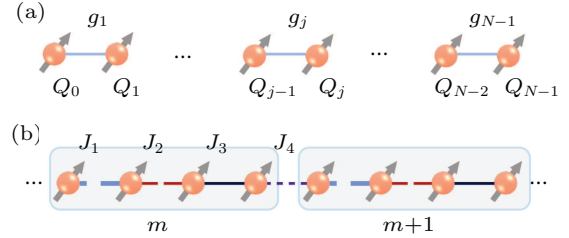


Fig. 1. (a) Schematic diagram of a qubit chain. Here, Q_j denotes the j th qubit, g_j is the coupling between neighboring qubits. (b) Schematic diagram of a quadrimeric superlattice with four qubits in each unit cell. J_1 , J_2 , and J_3 are the intra-cell couplings, whereas J_4 is the inter-cell coupling.

To demonstrate the topological properties of superlattice in superconducting circuits, here we focus on a superlattice qubit chain with four qubits in each unit cell denoted as $\{1, 2, 3, 4\}$, as shown in Fig. 1(b), which is known as the SSH₄ model. For such a quadrimeric lattice, the Hamiltonian reads

$$\begin{aligned} H &= \sum_{m=1}^M \left(J_1 \sigma_{m,1}^+ \sigma_{m,2}^- + J_2 \sigma_{m,2}^+ \sigma_{m,3}^- + J_3 \sigma_{m,3}^+ \sigma_{m,4}^- \right. \\ &\quad \left. + J_4 \sigma_{m,4}^+ \sigma_{m+1,1}^- + \text{H.c.} \right), \end{aligned} \quad (9)$$

where m is the unit cell index, M is the number of the unit cells, J_1 , J_2 , and J_3 denote the intracell qubit coupling strengths and J_4 is the intercell qubit coupling strength. For simplicity, we take $\hbar = 1$ and set J_1 as the energy scale.

Note that the Hamiltonian (9) describes an interacting spin chain. Here, we consider the single-excitation case, i.e., one of the qubits is excited to the excited state $|e\rangle$ and the others stay in the ground state $|g\rangle$.

3. Topological phase transition

To study the topological feature of the qubit superlattice, we rewrite the Hamiltonian (9) in the momentum space as

$$\tilde{H}(k) = \begin{pmatrix} 0 & h^\dagger \\ h & 0 \end{pmatrix} = \begin{pmatrix} 0 & 0 & J_1 & J_4 e^{-ik} \\ 0 & 0 & J_2 & J_3 \\ J_1 & J_2 & 0 & 0 \\ J_4 e^{ik} & J_3 & 0 & 0 \end{pmatrix}. \quad (10)$$

The eigenvalues are given by $E = \pm \sqrt{(J \pm \sqrt{J^2 - 4T})/2}$ with $J = J_1^2 + J_2^2 + J_3^2 + J_4^2$ and $T = (J_1 J_3)^2 + (J_2 J_4)^2 - 2J_1 J_2 J_3 J_4 \cos k$. It is found that there are four bands. If $J_1 J_3 = \pm J_2 J_4$, the gap between the middle bands is closed at $k = 0$ or $k = \pi$.

By introducing the matrix $\Gamma = I_2 \otimes \sigma_z$ with I_2 being the 2×2 identity matrix, one can verify that $\Gamma \tilde{H} + \tilde{H} \Gamma = 0$. Therefore, the SSH₄ model has a chiral symmetry and belongs to the same class of the SSH model, and the corresponding winding number can be obtained as follows:

$$w = \frac{1}{2\pi i} \int_0^{2\pi} dk z^{-1} \frac{dz}{dk}, \quad (11)$$

where $z = \det(h) = J_1 J_3 - J_2 J_4 e^{ik}$. Through a straightforward calculation, we have

$$w = \begin{cases} 1, & |J_1 J_3| < |J_2 J_4|, \\ 0, & |J_1 J_3| > |J_2 J_4|. \end{cases} \quad (12)$$

The winding number $w = 1$ (0) shows that the above qubit chain [Eq. (9)] is in the topologically nontrivial (trivial) phase.

For one-dimensional chiral symmetric systems, the winding number is an important topological invariant used to characterize the topological phase and can be measured through the dynamics of quantum state. That is, the winding number can be extracted from a time-dependent quantity—mean chiral displacement (MCD), which has been measured experimentally in cold atoms,^[46] photonic system,^[47] and superconducting qubit chain for the SSH-type model.^[28] For the SSH₄-type qubit chain, we define the chiral displacement operator as (see the appendix)

$$\hat{C} = \sum_x x (\hat{P}_{1x}^c - \hat{P}_{2x}^c + \hat{P}_{3x}^c - \hat{P}_{4x}^c), \quad (13)$$

with $\hat{P}_{ix}^c = |e\rangle_{ix} \langle e|$ ($i = 1, 2, 3, 4$). Here, x is the relabeled unit cell index with $\{x = \dots, -1, 0, 1, \dots\}$. Then the dynamics of the MCD is given as $\mathcal{C}(t) = \langle \psi(t) | \hat{C} | \psi(t) \rangle$. Here, $|\psi(t)\rangle = e^{-i\hat{H}t} |\psi(0)\rangle$ with $|\psi(0)\rangle$ being the initial state at time $t = 0$. The long-time average of the MCD, i.e., $\bar{C} = \lim_{T \rightarrow \infty} 1/T \int_0^T dt \mathcal{C}(t)$ can be used to characterize topological invariant.

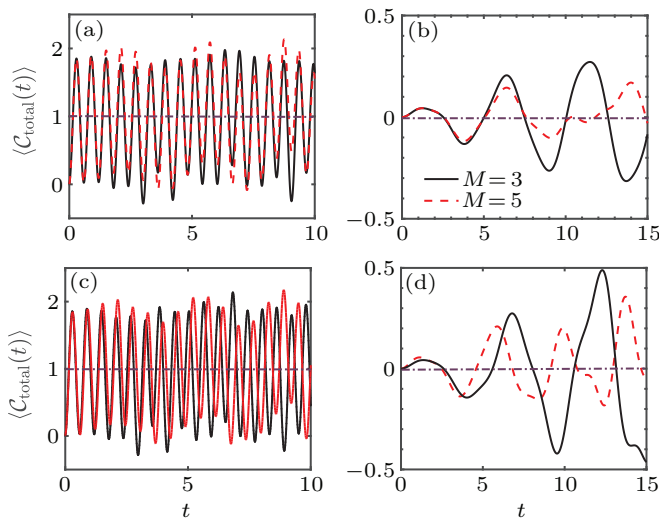


Fig. 2. (a) and (b) The dynamics of $\mathcal{C}_{\text{total}}(t)$ with $J_4 = 5$ (a) and $J_4 = 0.2$ (b), respectively. (c) and (d) The dynamics of $\langle \mathcal{C}_{\text{total}}(t) \rangle$ with $J_4 = 5$ (c) and $J_4 = 0.2$ (d), respectively. Here, $\langle \dots \rangle$ denotes the disorder-averaged $\mathcal{C}_{\text{total}}(t)$. The other parameters are chosen as $J_1 = J_2 = J_3$ and $W = 0.2$.

In order to detect the winding number for the SSH₄-type qubit chain, we consider two single excitation initial states localized on the central unit cell, i.e., $|\psi_1(0)\rangle = |gggg, \dots, eggg, \dots, gggg\rangle$ and $|\psi_3(0)\rangle = |gggg, \dots, ggge, \dots, gggg\rangle$. The corresponding MCDs are denoted as $\mathcal{C}_1(t)$ and $\mathcal{C}_3(t)$, respectively. The topological winding number can be extracted from the total MCD— $\mathcal{C}_{\text{total}}(t) = \mathcal{C}_1(t) + \mathcal{C}_3(t)$, that is,

$$w = \bar{\mathcal{C}}_{\text{total}}. \quad (14)$$

As shown in Figs. 2(a) and 2(b), we simulate $\mathcal{C}_{\text{total}}(t)$ for different configurations with $J_4 > J_1 (= J_2 = J_3)$ and $J_4 < J_1 (= J_2 = J_3)$, corresponding to topological non-trivial and trivial phases, respectively. It is clear that the curve of $\mathcal{C}_{\text{total}}(t)$ oscillates around 1 when $J_4 > J_1$, which gives the topological winding number $w = 1$. For $J_4 < J_1$, $\mathcal{C}_{\text{total}}(t)$ oscillates around the average values 0 corresponding to trivial phase with $w = 0$. These results show that the long time dynamics of the chiral operator [Eq. (13)] can be effectively characterized different topological phases for SSH₄-type qubit chain.

To demonstrate the robustness of the MCD, we add the disorder to each qubit couplings as $J_i^m = J_i + W \delta$, where W is the disorder strength and $\delta \in [-0.5, 0.5]$ is a random number. In Figs. 2(c) and 2(d), we show the disorder-averaged MCD $\langle \mathcal{C}_{\text{total}} \rangle$ by averaging $\mathcal{C}_{\text{total}}(t)$ over 30 independent disorder configurations for trivial and nontrivial phases. It can be seen that $\langle \mathcal{C}_{\text{total}} \rangle$ is robust to the weak disorder, maintaining oscillation center around 1 and 0 for $J_4 > J_1$ and $J_4 < J_1$, respectively.

4. Detecting of edge states

A hallmark feature of topological insulators is the topologically protected boundary states. For the two-band SSH model, it supports limited number (one or two) of topological edge states. However, the superlattice systems show richer topological features due to the multiple topologically nontrivial dispersion bands. To determine the existence of topological phases and edge states, it is convenient to analyze the symmetries of the Hamiltonian. For Hamiltonian (10), the system possesses inversion symmetry, i.e., $\mathcal{P}H(k)\mathcal{P}^{-1} = H(-k)$ with $\mathcal{P} = \sigma_x \otimes \sigma_x$ when $J_1 = J_3$. Figure 4(a) shows the energy spectrum with $J_1 = J_3$. It is clear that there are two zero-energy degenerate edge states in the middle gap for $J_4 > J_{4,0}$ ($= J_1 J_3 / J_2$), and there are two degenerate edge states for $J_4 > J_{4,1}$ ($= J_2$) in the upper and lower gaps. Such topological phases can be described by the Zak phase, which is defined as $\gamma_s = i \int_{-\pi}^{\pi} dk \langle \psi_{s,k} | \partial_k \psi_{s,k} \rangle$ with $\psi_{s,k}$ being the s th-Bloch-wave functions. For multiband systems, the topological properties of the n th band gap is characterized by the sum of Zak

phase of all the isolated bands below the corresponding band gap, i.e.,

$$\mathcal{Z}_n = \gamma_1 + \dots + \gamma_n. \quad (15)$$

In Figs. 3(a1)–3(a3), we plot the Zak phase \mathcal{Z}_n ($n = 1, 2, 3$) of the corresponding band gap of the SSH₄ model under the inversion symmetry. We find that \mathcal{Z}_n is quantized and can take the values zero or π , denoting the trivial and nontrivial topological phases, respectively. The nontrivial Zak phase implies that a pair of topologically protected edge states will appear at the boundaries of the system.

In the case of $J_1 \neq J_3$, the superlattice has no inversion symmetry. Figure 3(b) shows the energy spectrum and Figs. 3(b1)–3(b3) show the corresponding gap Zak phase \mathcal{Z}_n with $J_1 \neq J_3$. It can be seen that the Zak phase of the middle gap is quantized, and a pair of degenerate zero-energy edge state emerge for $J_4 > J_{4,2}$ ($= J_1 J_3 / J_2$). However, for the upper and lower gaps, the Zak phases $\mathcal{Z}_{1,3}$ are not quantized and vary continuously. The non-degenerate edge states emerge without experiencing a gap closing and reopening point, and they are not topological.

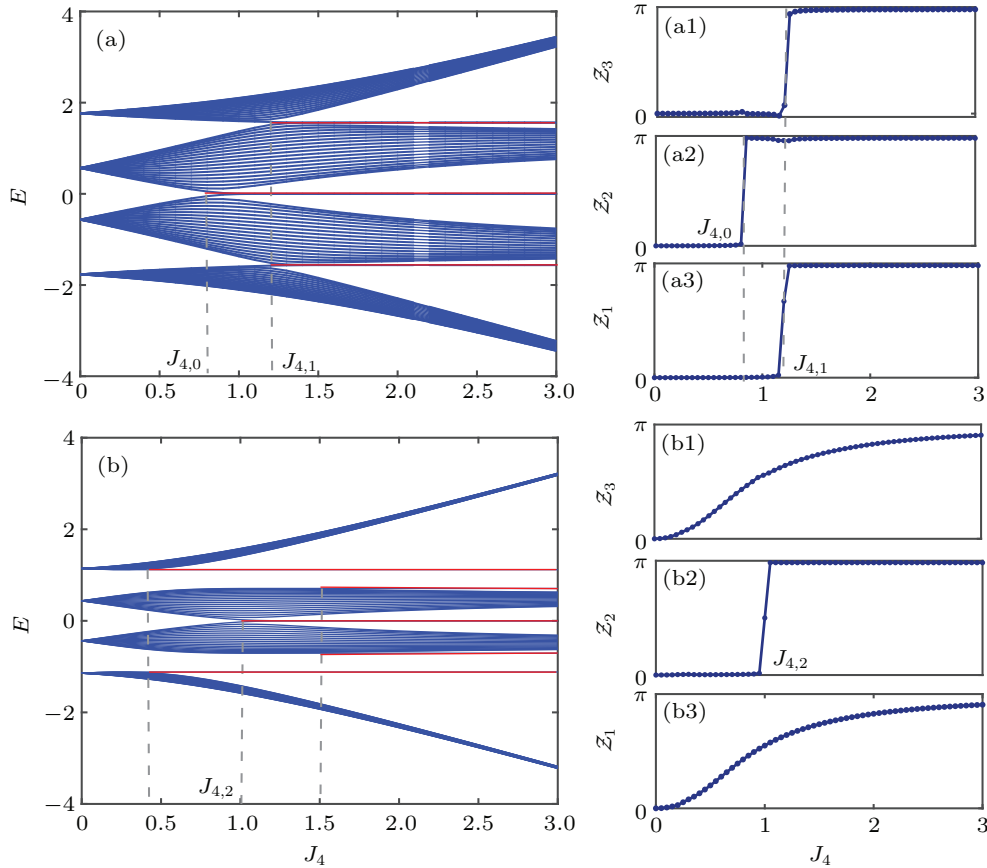


Fig. 3. (a) The energy spectrum with the inversion symmetry $\{J_1 = J_3 = 1, J_2 = 1.2\}$. (a1)–(a3) The corresponding band gap Zak phases \mathcal{Z}_n versus the inter-cell coupling J_4 . (b) The energy spectrum without inversion symmetry $\{J_1 = 1, J_3 = 0.5, J_2 = 0.5\}$. (b1)–(b3) The Zak phases corresponding to all band gaps.

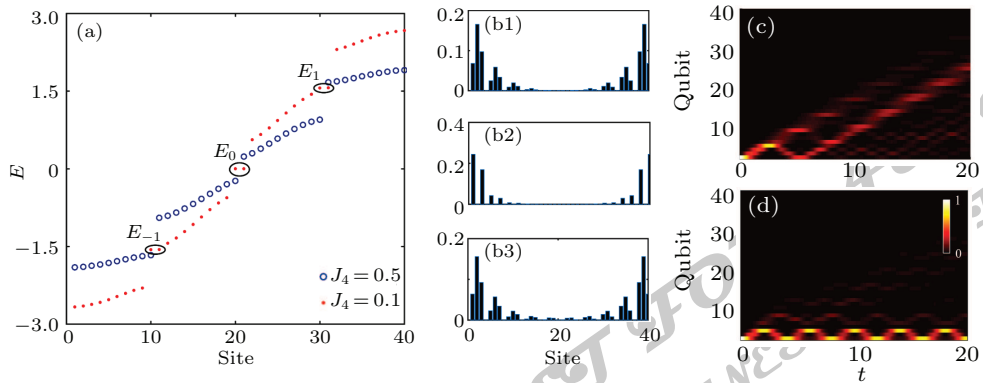


Fig. 4. (a) The energy spectrum with $J_4 = 0.5$ (blue circle) and $J_4 = 2$ (red dot). (b1)–(b3) The distribution of wave functions of the three pairs edge states indicated by circles in (a), respectively. (c) and (d) The time evolution of the single-excited state population for $J_4 = 0.5$ (a) and $J_4 = 2$ (b), respectively. The other parameters are chosen as $J_1 = J_3 = 1$ and $J_2 = 1.2$.

The above discussion shows that the number of topological edge states can be controlled by tuning the inter- and intra-cell couplings. The topological edge states can be detected by the dynamics of the single-excitation quantum state. As an example, in Fig. 4(a), we plot the energy spectrum with $J_4 = 0.5$ (blue circle) and $J_4 = 2$ (red dot). In the topological phase ($J_4 = 2$), there are three pairs of edge state in the gaps and the distribution wave functions of them are shown in Figs. 4(b1)–4(b3). Figures 4(c) and 4(d) show the time evolution of the single-excited state ($|\psi(0)\rangle = \sigma_1^+ |G\rangle$) population for $J_4 = 0.5$ and $J_4 = 2$, respectively. For the non-topological phase, the excited state spreads into the bulk over time, while in the topological phase with edge states, the wave-packet remains localized around the boundary unit cell.

5. Dynamics of interface state

Another important topological aspect is the existence of interface states between two topological distinct insulators. As shown schematically in Fig. 5(a), a topological interface (shaded region) can be created by combining two SSH₄-type qubit systems with different topological properties [e.g., in Fig. 5(a), the qubit array on the right (left) represents a topologically nontrivial (trivial) array with $J_4 < J_1 = J_2 = J_3$ ($J_4 > J_1 = J_2 = J_3$)]. The energy spectrum is shown in Fig. 5(b) with $\{J_{1,2,3} = 1, J_4 = 5\}$. There are three localized interface states existing in the gap, and the distribution of these three states are shown in Fig. 5(c).

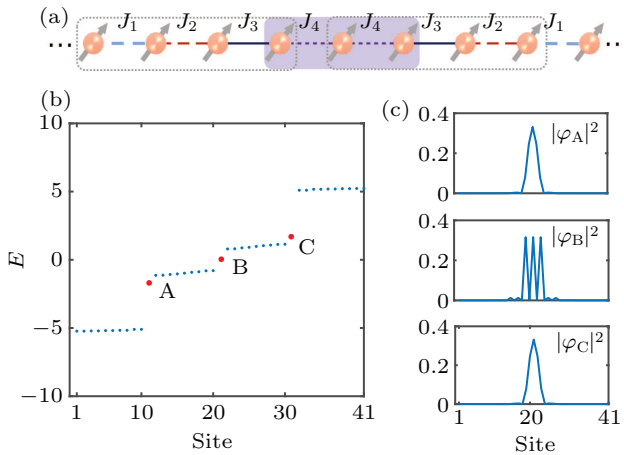


Fig. 5. (a) Schematic diagram of the two-coupled-qubit chain with different topological phases. The central shaded region denotes the interface. (b) The energy spectrum of the qubit configuration shown in (a). The red dots represent the interface states. (c) The distribution wave function of the interface states. The parameters are chosen are $J_1 = J_2 = J_3, J_4 = 5$ and $M = 10$.

To observe the dynamics of topological interface states, we excite the central qubit of the interface region [Fig. 5(a)]. Such an initial state has a large overlap with the wave function of the interface states and it will propagate in the qubit chain via the interface states. Compared with the localized defect state in the SSH-type qubit chain, the interface states

of superlattice exhibit exotic behaviors.^[37,39] Figures 6(a) and 6(b) show the time evolutions of single-excitation state population with $M = 4$ and $M = 2$, respectively. It is found that the dynamics of the single-excitation exhibits Bloch-like oscillation. Such breathing-like oscillation is due to the interference of topological interface states with different propagation constants, which is quite different from general Bloch oscillation with a linear potential.^[48] The results indeed indicate that the single-excited state is localized in the center interface region of the qubit chain, unambiguously demonstrate the existence of the topological interface states.

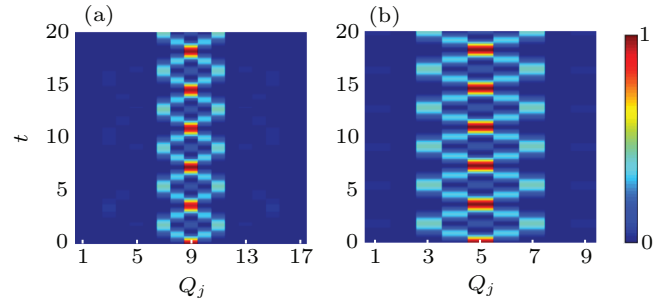


Fig. 6. Time evolutions of all qubit's excited state population with $M = 4$ (a) and $M = 2$ (b). The initial excitation is the central qubit of the interface region as shown in Fig. 5(a). The other parameters are the same as those in Fig. 5(b).

6. Conclusion

In summary, we have constructed one-dimensional superlattices in superconducting circuits with tunable coupling strengths. As an example, we consider the quadrimeric lattice. Such a multiband system shows richer topological properties than the dimeric case. Through the non-equilibrium dynamics of a single-qubit excitation state, we show that the topological winding number can be measured by a dynamical dependent quantity, i.e., mean chiral displacement, which takes zero for the trivial phase and 1 for the nontrivial phase. Moreover, we have demonstrated the existence of topological edge state under different parameters region. Finally, the stable Bloch-like oscillation of multiple interface states induced by the interference of them has been demonstrated. In the experiment, accurate single-shot readout techniques enable us to synchronously record the dynamics of all qubits and to observe the evolution of a single-excitation state. In addition, the physics presented here persists even for finite size, indicating the feasibility of experimental measurements. Note that similar physics can be extended to superlattices with arbitrary number of qubits in each unit cell. Our work potentially paves the way for exploring novel topological states of matter in controllable superconducting circuits.

Appendix A

Here, we derive the validity of the mean chiral displacement in our quadrimeric lattice.^[49] First, let us define the projectors $P_j = |\psi_j\rangle\langle\psi_j|$ and $Q = \sum_{j=1,2} Q_j = \sum_{j=1,2} (P_j - P_{-j})$,

where $|\psi_j\rangle$ ($j = \pm 1, \pm 2$) denotes the the eigenstate of the Bloch Hamiltonian (10) with energy E_j . These representations comes from the chiral symmetry where the eigenenergies and eigenstates satisfy $E_j = -E_{-j}$ and $\hat{\Gamma}|\psi_j\rangle = |\psi_{-j}\rangle$. The winding number can be computed through the integral over the Brillouin zone of the skew polarization $S = \sum_{j \in \text{occ}} S_j$, i.e., $w = \oint \frac{dk}{2\pi} S(k)$, where $S_j = i \langle \Gamma \psi_j | \psi'_j \rangle$ with $|\psi'_j\rangle = \partial_k |\psi_j\rangle$.

For a generic localized state $|\overline{\Psi}\rangle$, the mean chiral displacement ($\langle \hat{C}(t) \rangle \equiv \langle \hat{\Gamma} \cdot x(t) \rangle$) is given by

$$\langle \hat{\Gamma} \cdot x(t) \rangle_{\overline{\Psi}} = \oint \sum_{j=1,2} \frac{dk}{2\pi} \langle \Psi | U_t^\dagger \Gamma(i\partial_k) U_t | \Psi \rangle, \quad (\text{A1})$$

where $U_t = e^{-iHt}$ is the unitary evolution operator and $|\overline{\Psi}\rangle = \oint \frac{dk}{2\pi} |\Psi\rangle$. Through a simple calculation, we have

$$\begin{aligned} & P_j [U^{-t} \Gamma \partial_k U^t] P_{j'} \\ &= \delta_{j,-j'} \left[P_j \Gamma \partial_k \frac{e^{i2tE_j}}{2} + e^{i2tE_j} |\psi_j\rangle \langle \psi'_{-j}| \right] \\ & \quad + e^{it(E_j - E_{j'})} |\psi_j\rangle \langle \psi_{-j} | \psi'_{j'} \rangle \langle \psi'_{j'} | \\ &= \delta_{j,-j'} \left[P_j \Gamma \partial_k \frac{e^{i2tE_j}}{2} + e^{i2tE_j} |\psi_j\rangle \langle \psi'_{-j}| \right] \\ & \quad - e^{it(E_j - E_{j'})} |\psi_j\rangle \langle \psi'_{-j} | P_{j'}. \end{aligned} \quad (\text{A2})$$

For simplicity, we define the projector on the subspace of chiral-partner eigenstates, $R_j = P_j + P_{-j}$. Equation (A2) multiplied by i gives the sum of two terms, a term T_1 which acts in the subspace of chiral partner states with $|j| = |j'|$ and a term T_2 which acts in the subspace of the states with $|j| \neq |j'|$. Using $R_j \Gamma = \Gamma_j$, $\partial_k \Gamma = 0$ and $iQ_j S_j = \partial_k (Q_j \Gamma) / 2$, these two terms become

$$\begin{aligned} T_1 &= \sum_{j=1}^{D/2} S_j [1 - \cos(2E_j t)] R_j + i R_j \Gamma \partial_k \left[\frac{\cos(2E_j t)}{2} \right] \\ & \quad - Q_j \Gamma \partial_k \left[\frac{\sin(2E_j t)}{2} \right] - i Q_j S_j \sin(2E_j t) \\ &= \sum_{j=1}^{D/2} S_j [1 - \cos(2E_j t)] R_j \\ & \quad + \partial_k \left[i \Gamma_j \frac{\cos(2E_j t)}{2} - Q_j \Gamma \frac{\sin(2E_j t)}{2} \right], \quad (\text{A3}) \\ T_2 &= \sum_{j,j'=\pm 1, \pm 2 (|j| \neq |j'|)} \langle \psi_{-j} | \psi'_{j'} \rangle |\psi_j\rangle \langle \psi'_{j'} | e^{it(E_j - E_{j'})}. \end{aligned} \quad (\text{A4})$$

It is obvious that the term T_2 is purely oscillatory, so it will average to zero in the long time limit. Considering $\langle \Gamma \rangle_{\psi_j} = 0$ and $\langle Q \Gamma \rangle_{\psi_j} = 0$, we have

$$\langle \hat{\Gamma} \cdot x(t) \rangle_{\overline{\Psi}} = \oint \frac{dk}{2\pi} \left\langle T_2 + \sum_{j=1,2} S_j [1 - \cos(2tE_j)] R_j \right\rangle_{\Psi}. \quad (\text{A5})$$

For the state $|\overline{\psi_j}\rangle (= \oint \frac{dk}{2\pi} |\psi_j\rangle)$ and $|\overline{\Gamma_j}\rangle (= [\text{sgn}(j)] |\overline{\psi_j}\rangle +$

$|\overline{\psi_{-j}}\rangle / \sqrt{2}$), we have $\langle T_2 \rangle_{\psi_j} = \langle T_2 \rangle_{\Gamma_j} = 0$ and $\langle R_j \rangle_{\psi_{j'}} = \langle R_j \rangle_{\Gamma_{j'}} = \delta_{jj'}$, then obtain

$$\begin{aligned} \sum_{j=1,2} \langle \hat{\Gamma} \cdot x \rangle_{\overline{\Gamma_j}} &= \sum_{j=1,2} \langle \hat{\Gamma} \cdot x \rangle_{\overline{\psi_j}} \\ &= \oint \frac{dk}{2\pi} \sum_{j=1}^{D/2} S_j [1 - \cos(2tE_j)] \\ &= \frac{w}{2} + \text{osc.}, \end{aligned} \quad (\text{A6})$$

where osc. denotes the oscillatory term which tends to zero in the long time limit.

Acknowledgements

Project supported by the National Natural Science Foundation of China (Grant Nos. 12034012, 12074232, 12125406, and 11804204) and 1331KSC.

References

- [1] Koch J, Yu T M, Gambetta J, Houck A A, Schuster D I, Majer J, Blais A, Devoret M H, Girvin S M and Schoelkopf R J 2007 *Phys. Rev. A* **76** 042319
- [2] Gu X, Kockum A F, Miranowicz A, Liu Y and Nori F 2017 *Phys. Rep.* **718** 1
- [3] Blais A, Grimsmo A L, Girvin S M and Wallraff A 2021 *Rev. Mod. Phys.* **93** 025005
- [4] Wang Z, Bao Z, Wu Y, Li Y, Ma C, Cai T, Song Y, Zhang H and Duan L 2021 *Chin. Phys. Lett.* **38** 110303
- [5] Li D Y, Chu J, Zheng W, Lan D, Zhao J, Li S X, Tan X S and Yu Y 2021 *Chin. Phys. B* **30** 070308
- [6] Ye Y, Cao S, Wu Y, Chen X, Zhu Q, Li S, Chen F, Gong M, Zha C, Huang H L, Zhao Y, Wang S, Guo S, Qian H, Liang F, Lin J, Xu Y, Guo C, Sun L, Li N, Deng H, Zhu X and Pan J W 2021 *Chin. Phys. Lett.* **38** 100301
- [7] Houck A A, Tüeci H E and Koch J 2012 *Nat. Phys.* **8** 292
- [8] Georgescu I M, Ashhab S and Nori F 2014 *Rev. Mod. Phys.* **86** 153
- [9] Xue Z Y and Hu Y 2021 *Adv. Quantum Technol.* **4** 2100017
- [10] He K, Geng X, Huang R, Liu J and Chen W 2021 *Chin. Phys. B* **30** 080304
- [11] Jin J, Rossini D, Fazio R, Leib M and Hartmann M J 2013 *Phys. Rev. Lett.* **110** 163605
- [12] Ye Y, Ge Z Y, Wu Y, Wang S, Gong M, Zhang Y R, Zhu Q, Yang R, Li S, Liang F, Lin J, Xu Y, Guo C, Sun L, Cheng C, Ma N, Meng Z Y, Deng H, Rong H, Lu C Y, Peng C Z, Fan H, Zhu X and Pan J W 2019 *Phys. Rev. Lett.* **123** 050502
- [13] Kounalakis M, Dickel C, Bruno A, Langford N K and Steele G A 2018 *npj Quantum Inf.* **4** 38
- [14] Roushan P, et al. 2017 *Science* **358** 1175
- [15] Xu K, Chen J J, Zeng Y, Zhang Y R, Song C, Liu W, Guo Q, Zhang P, Xu D, Deng H, Huang K, Wang H, Zhu X, Zheng D and Fan H 2018 *Phys. Rev. Lett.* **120** 050507
- [16] Orell T, Michailidis A A, Serbyn M and Silveri M 2019 *Phys. Rev. B* **100** 134504
- [17] Guo Q, Cheng C, Sun Z H, Song Z, Li H, Wang Z, Ren W, Dong H, Zheng D, Zhang Y R, Mondaini R, Fan H and Wang H 2021 *Nat. Phys.* **17** 234
- [18] Gong M, Neto G D, Zha C, Wu Y, Rong H, Ye Y, Li S, Zhu Q, Wang S, Zhao Y, Liang F, Lin J, Xu Y, Peng C Z, Deng H, Bayat A, Zhu X and Pan J W 2021 *Phys. Rev. Res.* **3** 033043
- [19] Gong M, Wang S, Zha C, Chen M C, Huang H L, Wu Y, Zhu Q, Zhao Y, Li S, Guo S, Qian H, Ye Y, Chen F, Ying C, Yu J, Fan D, Wu D, Su H, Deng H, Rong H, Zhang K, Cao S, Lin J, Xu Y, Sun L, Guo C, Li N, Liang F, Bastidas V M, Nemoto K, Munro W J, Huo Y H, Lu C Y, Peng C Z, Zhu X and Pan J W 2021 *Science* **372** 948
- [20] Yan Z, Zhang Y R, Gong M, Wu Y, Zheng Y, Li S, Wang C, Liang F, Lin J, Xu Y, Guo C, Sun L, Peng C Z, Xia K, Deng H, Rong H, You J Q, Nori F, Fan H, Zhu X and Pan J W 2019 *Science* **364** 753

- [21] Flurin E, Ramasesh V V, Hacohen-Gourgy S, Martin L S, Yao N Y and Siddiqi I 2017 *Phys. Rev. X* **7** 031023
- [22] Xu K, Sun Z, Liu W, Zhang Y R, Li H, Dong H, Ren W, Zhang P, Nori F, Zheng D, Fan H and Wang H 2020 *Sci. Adv.* **6** eaba4935
- [23] Ramasesh V V, Flurin E, Rudner M, Siddiqi I and Yao N Y 2017 *Phys. Rev. Lett.* **118** 130501
- [24] Mei F, Chen G, Tian L, Zhu S L and Jia S 2018 *Phys. Rev. A* **98** 012331
- [25] Hu K X, Chen C, Qi L, Cui W X, Zhang S and Wang H F 2021 *Phys. Rev. A* **104** 023707
- [26] Wu C, Guan X, Fan J, Chen G and Jia S 2021 *Phys. Rev. A* **104** 022601
- [27] Niu J, Yan T, Zhou Y, Tao Z, Li X, Liu W, Zhang L, Liu S, Yan Z, Chen Y and Yu D 2021 *Sci. Bull.* **66** 1168
- [28] Cai W, Han J, Mei F, Xu Y, Ma Y, Li X, Wang H, Song Y P, Xue Z Y, Yin Z Q, Jia S and Sun L 2019 *Phys. Rev. Lett.* **123** 080501
- [29] Li L, Xu Z and Chen S 2014 *Phys. Rev. B* **89** 085111
- [30] Bandyopadhyay S, Bhattacharya U and Dutta A 2019 *Phys. Rev. B* **100** 054305
- [31] Vyas V M and Roy D 2021 *Phys. Rev. B* **103** 075441
- [32] Bandyopadhyay S and Dutta A 2019 *Phys. Rev. B* **100** 144302
- [33] Liu J S, Han Y Z and Liu C S 2019 *Chin. Phys. B* **28** 100304
- [34] Liu J S, Han Y Z and Liu C S 2020 *Chin. Phys. B* **29** 010302
- [35] Yao S and Wang Z 2018 *Phys. Rev. Lett.* **121** 086803
- [36] Wang X R, Guo C X, Du Q and Kou S P 2020 *Chin. Phys. Lett.* **37** 117303
- [37] Midya B and Feng L 2018 *Phys. Rev. A* **98** 043838
- [38] Xie D, Gou W and Xiao T 2019 *npj Quantum Inf.* **5** 55
- [39] Wang Y, Lu Y H, Gao J, Chang Y J, Tang H and Jin X M 2019 *Phys. Rev. B* **103** 014110
- [40] Stefano L 2019 *Opt. Lett.* **44** 2530
- [41] Li X, Ma Y, Han J, Chen T, Xu Y, Cai W, Wang H, Song Y P, Xue Z Y, Yin Z Q and Sun L 2018 *Phys. Rev. Appl.* **10** 054009
- [42] Reagor M, Osborn C, Tezak N, *et al.* 2018 *Sci. Adv.* **4** eaao3603
- [43] Li J W, Wu C W and Dai H Y 2011 *Chin. Phys. Lett.* **28** 090302
- [44] Chen T, Shen P and Xue Z Y 2020 *Phys. Rev. Applied* **14** 034038
- [45] Guan X, Feng Y L, Xue Z Y, Chen G and Jia S 2020 *Phys. Rev. A* **102** 032610
- [46] Meier E J, An F A, Dauphin A, Maffei M, Massignan P, Hughes T L and Gadway B 2018 *Science* **362** 929
- [47] Cardano F, D'Errico A, Dauphin A, Maffei M, Piccirillo B, Lisio C D, Filippis G D, Cataudella V, Santamato E, Marrucci L, Lewenstein M and Massignan P 2017 *Nat. Commun.* **8** 15516
- [48] Guo X Y, Ge Z Y, Li H, Wang Z, Zhang Y R, Song P, Xiang Z, Song X, Jin Y, Lu L, Xu K, Zheng D and Fan H 2021 *npj Quantum Inf.* **7** 51
- [49] Maffei M, Dauphin A, Cardano F, Lewenstein M and Massignan P 2018 *New J. Phys.* **20** 013023

JUST FOR AUTHORS
— CHINESE PHYSICS B

Chinese Physics B

Volume 31 Number 8 August 2022

Contents

TOPICAL REVIEW — Celebrating 30 Years of *Chinese Physics B*

080301 Exploring Majorana zero modes in iron-based superconductors

Geng Li, Shiyu Zhu, Peng Fan, Lu Cao and Hong-Jun Gao

085202 Fundamental study towards a better understanding of low pressure radio-frequency plasmas for industrial applications

Yong-Xin Liu, Quan-Zhi Zhang, Kai Zhao, Yu-Ru Zhang, Fei Gao, Yuan-Hong Song and You-Nian Wang

087104 Mottness, phase string, and high- T_c superconductivity

Jing-Yu Zhao and Zheng-Yu Weng

087301 Recent advances of defect-induced spin and valley polarized states in graphene

Yu Zhang, Lianguang Jia, Yaoyao Chen, Lin He and Yeliang Wang

087506 Magnetic van der Waals materials: Synthesis, structure, magnetism, and their potential applications

Zhongchong Lin, Yuxuan Peng, Baochun Wu, Changsheng Wang, Zhaochu Luo and Jinbo Yang

087507 Progress and challenges in magnetic skyrmionics

Haifeng Du and Xiangrong Wang

088106 Photon-interactions with perovskite oxides

Hongbao Yao, Er-Jia Guo, Chen Ge, Can Wang, Guozhen Yang and Kuijuan Jin

089101 Evolution of electrical conductivity and semiconductor to metal transition of iron oxides at extreme conditions

Yukai Zhuang and Qingyang Hu

089401 Collisionless magnetic reconnection in the magnetosphere

Quanming Lu, Huishan Fu, Rongsheng Wang and San Lu

DATA PAPER

080101 New experimental measurement of $^{nat}\text{Se}(n, \gamma)$ cross section between 1 eV to 1 keV at the CSNS Back-n facility

Xin-Rong Hu, Long-Xiang Liu, Wei Jiang, Jie Ren, Gong-Tao Fan, Hong-Wei Wang, Xi-Guang Cao, Long-Long Song, Ying-Du Liu, Yue Zhang, Xin-Xiang Li, Zi-Rui Hao, Pan Kuang, Xiao-He Wang, Ji-Feng Hu, Bing Jiang, De-Xin Wang, Suyalatu Zhang, Zhen-Dong An, Yu-Ting Wang, Chun-Wang Ma, Jian-Jun He, Jun Su, Li-Yong Zhang, Yu-Xuan Yang, Sheng Jin and Kai-Jie Chen

(Continued on the Bookbinding Inside Back Cover)

083101 Relativistic calculations on the transition electric dipole moments and radiative lifetimes of the spin-forbidden transitions in the antimony hydride molecule

Yong Liu, Lu-Lu Li, Li-Dan Xiao and Bing Yan

083401 Integral cross sections for electron impact excitations of argon and carbon dioxide

Shu-Xing Wang and Lin-Fan Zhu

087501 Magnetic properties of oxides and silicon single crystals

Zhong-Xue Huang, Rui Wang, Xin Yang, Hao-Feng Chen and Li-Xin Cao

INSTRUMENTATION AND MEASUREMENT

084207 A 658-W VCSEL-pumped rod laser module with 52.6% optical efficiency

Xue-Peng Li, Jing Yang, Meng-Shuo Zhang, Tian-Li Yang, Xiao-Jun Wang and Qin-Jun Peng

088401 Design and high-power test of 800-kW UHF klystron for CEPC

Ou-Zheng Xiao, Shigeki Fukuda, Zu-Sheng Zhou, Un-Nisa Zaib, Sheng-Chang Wang, Zhi-Jun Lu, Guo-Xi Pei, Munawar Iqbal and Dong Dong

RAPID COMMUNICATION

086801 Two-dimensional Sb cluster superlattice on Si substrate fabricated by a two-step method

Runxiao Zhang, Zi Liu, Xin Hu, Kun Xie, Xinyue Li, Yumin Xia and Shengyong Qin

087102 Effect of f-c hybridization on the $\gamma \rightarrow \alpha$ phase transition of cerium studied by lanthanum doping

Yong-Huan Wang, Yun Zhang, Yu Liu, Xiao Tan, Ce Ma, Yue-Chao Wang, Qiang Zhang, Deng-Peng Yuan, Dan Jian, Jian Wu, Chao Lai, Xi-Yang Wang, Xue-Bing Luo, Qiu-Yun Chen, Wei Feng, Qin Liu, Qun-Qing Hao, Yi Liu, Shi-Yong Tan, Xie-Gang Zhu, Hai-Feng Song and Xin-Chun Lai

087302 Precisely controlling the twist angle of epitaxial MoS₂/graphene heterostructure by AFM tip manipulation

Jiahao Yuan, Mengzhou Liao, Zhiheng Huang, Jinpeng Tian, Yanbang Chu, LuoJun Du, Wei Yang, Dongxia Shi, Rong Yang and Guangyu Zhang

087401 Conservation of the particle-hole symmetry in the pseudogap state in optimally-doped Bi₂Sr₂CuO_{6+ δ} superconductor

Hongtao Yan, Qiang Gao, Chunyao Song, Chaohui Yin, Yiwen Chen, Fengfeng Zhang, Feng Yang, Shenjin Zhang, Qinjun Peng, Guodong Liu, Lin Zhao, Zuyan Xu and X. J. Zhou

088105 Monolayer MoS₂ of high mobility grown on SiO₂ substrate by two-step chemical vapor deposition

Jia-Jun Ma, Kang Wu, Zhen-Yu Wang, Rui-Song Ma, Li-Hong Bao, Qing Dai, Jin-Dong Ren and Hong-Jun Gao

GENERAL

080201 Robustness measurement of scale-free networks based on motif entropy

Yun-Yun Yang, Biao Feng, Liao Zhang, Shu-Hong Xue, Xin-Lin Xie and Jian-Rong Wang

- 080202 Quantum fields presentation and generating functions of symplectic Schur functions and symplectic universal characters**
Denghui Li, Fei Wang and Zhaowen Yan
- 080203 Green's function Monte Carlo method combined with restricted Boltzmann machine approach to the frustrated J_1 - J_2 Heisenberg model**
He-Yu Lin, Rong-Qiang He and Zhong-Yi Lu
- 080204 Evolution of donations on scale-free networks during a COVID-19 breakout**
Xian-Jia Wang and Lin-Lin Wang
- 080302 Hard-core Hall tube in superconducting circuits**
Xin Guan, Gang Chen, Jing Pan and Zhi-Guo Gui
- 080303 Finite-key analysis of practical time-bin high-dimensional quantum key distribution with afterpulse effect**
Yu Zhou, Chun Zhou, Yang Wang, Yi-Fei Lu, Mu-Sheng Jiang, Xiao-Xu Zhang and Wan-Su Bao
- 080304 Purification in entanglement distribution with deep quantum neural network**
Jin Xu, Xiaoguang Chen, Rong Zhang and Hanwei Xiao
- 080305 Non-universal Fermi polaron in quasi two-dimensional quantum gases**
Yue-Ran Shi, Jin-Ge Chen, Kui-Yi Gao and Wei Zhang
- 080306 Achieving ultracold Bose-Fermi mixture of ^{87}Rb and ^{40}K with dual dark magnetic-optical-trap**
Jie Miao, Guoqi Bian, Biao Shan, Liangchao Chen, Zengming Meng, Pengjun Wang, Lianghui Huang and Jing Zhang
- 080307 Direct measurement of two-qubit phononic entangled states via optomechanical interactions**
A-Peng Liu, Liu-Yong Cheng, Qi Guo, Shi-Lei Su, Hong-Fu Wang and Shou Zhang
- 080501 Inertial focusing and rotating characteristics of elliptical and rectangular particle pairs in channel flow**
Pei-Feng Lin, Xiao Hu and Jian-Zhong Lin
- 080502 Characteristics of piecewise linear symmetric tri-stable stochastic resonance system and its application under different noises**
Gang Zhang, Yu-Jie Zeng and Zhong-Jun Jiang
- 080503 Hyperparameter on-line learning of stochastic resonance based threshold networks**
Weijin Li, Yuhao Ren and Fabing Duan
- 080504 Synchronously scrambled diffuse image encryption method based on a new cosine chaotic map**
Xiaopeng Yan, Xingyuan Wang and Yongjin Xian
- 080505 Power-law statistics of synchronous transition in inhibitory neuronal networks**
Lei Tao and Sheng-Jun Wang

- 080506 Oscillation properties of matter–wave bright solitons in harmonic potentials**
Shu-Wen Guan, Ling-Zheng Meng and Li-Chen Zhao
- 080507 Effect of astrocyte on synchronization of thermosensitive neuron–astrocyte minimum system**
Yi-Xuan Shan, Hui-Lan Yang, Hong-Bin Wang, Shuai Zhang, Ying Li and Gui-Zhi Xu
- 080508 Exponential sine chaotification model for enhancing chaos and its hardware implementation**
Rui Wang, Meng-Yang Li and Hai-Jun Luo
- 080701 Ionospheric vertical total electron content prediction model in low-latitude regions based on long short-term memory neural network**
Tong-Bao Zhang, Hui-Jian Liang, Shi-Guang Wang and Chen-Guang Ouyang

ATOMIC AND MOLECULAR PHYSICS

- 083102 Dynamic polarizabilities of the clock states of Al^+**
Yuan-Fei Wei, Zhi-Ming Tang, Cheng-Bin Li, Yang Yang, Ya-Ming Zou, Kai-Feng Cui and Xue-Ren Huang
- 083103 Effect of conical intersection of benzene on non-adiabatic dynamics**
Duo-Duo Li and Song Zhang
- 083301 Nuclear dissociation after the $\text{O } 1s \rightarrow ({}^4\Sigma_u^-)3s\sigma$ excitation in O_2 molecules**
Bocheng Ding, Ruichang Wu, Yunfei Feng and Xiaojing Liu
- 083402 Elastic electron scattering with CH_2Br_2 and CCl_2Br_2 : The role of the polarization effects**
Xiaoli Zhao and Kedong Wang

ELECTROMAGNETISM, OPTICS, ACOUSTICS, HEAT TRANSFER, CLASSICAL MECHANICS, AND FLUID DYNAMICS

- 084101 Design method of reusable reciprocal invisibility and phantom device**
Cheng-Fu Yang, Li-Jun Yun and Jun-Wei Li
- 084201 Imaging a periodic moving/state-changed object with Hadamard-based computational ghost imaging**
Hui Guo, Le Wang and Sheng-Mei Zhao
- 084202 Orthogonal-triangular decomposition ghost imaging**
Jin-Fen Liu, Le Wang and Sheng-Mei Zhao
- 084203 Spatial and spectral filtering of tapered lasers by using tapered distributed Bragg reflector grating**
Jing-Jing Yang, Jie Fan, Yong-Gang Zou, Hai-Zhu Wang and Xiao-Hui Ma
- 084204 Optical fiber FBG linear sensing systems for the on-line monitoring of airborne high temperature air duct leakage**
Qinyu Wang, Xinglin Tong, Cui Zhang, Chengwei Deng, Siyu Xu and Jingchuang Wei

- 084205 Numerical study of converting beat-note signals of dual-frequency lasers to optical frequency combs by optical injection locking of semiconductor lasers**
Chenhao Liu, Haoshu Jin, Hui Liu and Jintao Bai
- 084206 A 45- μ J, 10-kHz, burst-mode picosecond optical parametric oscillator synchronously pumped at a second harmonic cavity**
Chao Ma, Ke Liu, Yong Bo, Zhi-Min Wang, Da-Fu Cui and Qin-Jun Peng
- 084208 High sensitivity dual core photonic crystal fiber sensor for simultaneous detection of two samples**
Pibin Bing, Guifang Wu, Qing Liu, Zhongyang Li, Lian Tan, Hongtao Zhang and Jianquan Yao
- 084209 High power supercontinuum generation by dual-color femtosecond laser pulses in fused silica**
Saba Zafar, Dong-Wei Li, Acner Camino, Jun-Wei Chang and Zuo-Qiang Hao
- 084210 Dynamically tunable multiband plasmon-induced transparency effect based on graphene nanoribbon waveguide coupled with rectangle cavities system**
Zi-Hao Zhu, Bo-Yun Wang, Xiang Yan, Yang Liu, Qing-Dong Zeng, Tao Wang and Hua-Qing Yu
- 084301 Three-dimensional coupled-mode model and characteristics of low-frequency sound propagation in ocean waveguide with seamount topography**
Ya-Xiao Mo, Chao-Jin Zhang, Li-Cheng Lu and Sheng-Ming Guo
- 084302 Sound-transparent anisotropic media for backscattering-immune wave manipulation**
Wei-Wei Kan, Qiu-Yu Li and Lei Pan
- 084701 Effect of pressure evolution on the formation enhancement in dual interacting vortex rings**
Jianing Dong, Yang Xiang, Hong Liu and Suyang Qin
- 084702 Drop impact on substrates with heterogeneous stiffness**
Yang Cheng, Jian-Gen Zheng, Chen Yang, Song-Lei Yuan, Guo Chen and Li-Yu Liu
- 084703 Physical aspects of magnetized Jeffrey nanomaterial flow with irreversibility analysis**
Fazal Haq, Muhammad Ijaz Khan, Sami Ullah Khan, Khadijah M Abualnaja and M A El-Shorbagy
- PHYSICS OF GASES, PLASMAS, AND ELECTRIC DISCHARGES**
- 085201 Combination of spark discharge and nanoparticle-enhanced laser-induced plasma spectroscopy**
Qing-Xue Li, Dan Zhang, Yuan-Fei Jiang, Su-Yu Li, An-Min Chen and Ming-Xing Jin
- CONDENSED MATTER: STRUCTURAL, MECHANICAL, AND THERMAL PROPERTIES**
- 086101 Substitutions of vertex configuration of Ammann–Beenker tiling in framework of Ammann lines**
Jia-Rong Ye, Wei-Shen Huang and Xiu-Jun Fu

- 086102 Radiation effects of electrons on multilayer FePS₃ studied with laser plasma accelerator**
Meng Peng, Jun-Bo Yang, Hao Chen, Bo-Yuan Li, Xu-Lei Ge, Xiao-Hu Yang, Guo-Bo Zhang and Yan-Yun Ma
- 086103 Synthesis of hexagonal boron nitride films by dual temperature zone low-pressure chemical vapor deposition**
Zhi-Fu Zhu, Shao-Tang Wang, Ji-Jun Zou, He Huang, Zhi-Jia Sun, Qing-Lei Xiu, Zhong-Ming Zhang, Xiu-Ping Yue, Yang Zhang, Jin-Hui Qu and Yong Gan
- 086104 Core structure and Peierls stress of the 90° dislocation and the 60° dislocation in aluminum investigated by the fully discrete Peierls model**
Hao Xiang, Rui Wang, Feng-Lin Deng and Shao-Feng Wang
- 086105 Theoretical and experimental studies on high-power laser-induced thermal blooming effect in chamber with different gases**
Xiangyizheng Wu, Jian Xu, Keling Gong, Chongfeng Shao, Yang Kou, Yuxuan Zhang, Yong Bo and Qinjun Peng
- 086106 Angular dependence of proton-induced single event transient in silicon-germanium heterojunction bipolar transistors**
Jianan Wei, Yang Li, Wenlong Liao, Fang Liu, Yonghong Li, Jiancheng Liu, Chaohui He and Gang Guo
- 086107 First-principles study of a new BP₂ two-dimensional material**
Zhizheng Gu, Shuang Yu, Zhirong Xu, Qi Wang, Tianxiang Duan, Xinxin Wang, Shijie Liu, Hui Wang and Hui Du
- 086108 Spatial correlation of irreversible displacement in oscillatory-sheared metallic glasses**
Shiheng Cui, Huashan Liu and Hailong Peng
- 086201 Ru thickness-dependent interlayer coupling and ultrahigh FMR frequency in Fe-CoB/Ru/FeCoB sandwich trilayers**
Le Wang, Zhao-Xuan Jing, Ao-Ran Zhou and Shan-Dong Li
- 086401 Nonvanishing optimal noise in cellular automaton model of self-propelled particles**
Guang-Le Du and Fang-Fu Ye
- 086802 Effects of oxygen concentration and irradiation defects on the oxidation corrosion of body-centered-cubic iron surfaces: A first-principles study**
Zhiqiang Ye, Yawei Lei, Jingdan Zhang, Yange Zhang, Xiangyan Li, Yichun Xu, Xuebang Wu, C. S. Liu, Ting Hao and Zhiguang Wang
- CONDENSED MATTER: ELECTRONIC STRUCTURE, ELECTRICAL, MAGNETIC, AND OPTICAL PROPERTIES**
- 087101 Modulation of Schottky barrier in XSi₂N₄/graphene (X = Mo and W) heterojunctions by biaxial strain**
Qian Liang, Xiang-Yan Luo, Yi-Xin Wang, Yong-Chao Liang and Quan Xie

- 087103 Tailored martensitic transformation and enhanced magnetocaloric effect in all-*d*-metal Ni₃₅Co₁₅Mn₃₃Fe₂Ti₁₅ alloy ribbons**
Yong Li, Liang Qin, Hongguo Zhang and Lingwei Li
- 087303 Analytical formula describing the non-saturating linear magnetoresistance in inhomogeneous conductors**
Shan-Shan Chen, Yang Yang and Fan Yang
- 087502 Magnetic properties of a mixed spin-3/2 and spin-2 Ising octahedral chain**
Xiao-Chen Na, Nan Si, Feng-Ge Zhang and Wei Jiang
- 087503 Exchange-coupling-induced fourfold magnetic anisotropy in CoFeB/FeRh bilayer grown on SrTiO₃(001)**
Qingrong Shao, Jing Meng, Xiaoyan Zhu, Yali Xie, Wenjuan Cheng, Dongmei Jiang, Yang Xu, Tian Shang and Qingfeng Zhan
- 087504 Electromagnetic wave absorption properties of Ba(CoTi)_xFe_{12-2x}O₁₉@BiFeO₃ in hundreds of megahertz band**
Zhi-Biao Xu, Zhao-Hui Qi, Guo-Wu Wang, Chang Liu, Jing-Hao Cui, Wen-Liang Li and Tao Wang
- 087505 Low-temperature heat transport of the zigzag spin-chain compound SrEr₂O₄**
Liguo Chu, Shuangkui Guang, Haidong Zhou, Hong Zhu and Xuefeng Sun
- 087801 High-dispersive mirror for pulse stretcher in femtosecond fiber laser amplification system**
Wenjia Yuan, Weidong Shen, Chen Xie, Chenying Yang and Yueguang Zhang
- 087802 Improving efficiency of inverted perovskite solar cells via ethanolamine-doped PEDOT:PSS as hole transport layer**
Zi-Jun Wang, Jia-Wen Li, Da-Yong Zhang, Gen-Jie Yang and Jun-Sheng Yu
- 087803 Enhanced photoluminescence of monolayer MoS₂ on stepped gold structure**
Yu-Chun Liu, Xin Tan, Tian-Ci Shen and Fu-Xing Gu
- 087804 Dual-channel tunable near-infrared absorption enhancement with graphene induced by coupled modes of topological interface states**
Zeng-Ping Su, Tong-Tong Wei and Yue-Ke Wang
- INTERDISCIPLINARY PHYSICS AND RELATED AREAS OF SCIENCE AND TECHNOLOGY**
- 088101 Degradation mechanisms for a-InGaZnO thin-film transistors functioning under simultaneous DC gate and drain biases**
Tianyuan Song, Dongli Zhang, Mingxiang Wang and Qi Shan
- 088102 Longitudinal conductivity in ABC-stacked trilayer graphene under irradiating of linearly polarized light**
Guo-Bao Zhu, Hui-Min Yang and Jie Yang

- 088103 Multiple bottle beams based on metasurface optical field modulation and their capture of multiple atoms**
Xichun Zhang, Wensheng Fu, Jinguang Wang, Shi-Yang Fu, Si-Han He, Hai-Bo Lv, Chong Zhang, Xin Zhao, Weiyan Li and He Zhang
- 088104 Determination of band alignment between GaO_x and boron doped diamond for a selective-area-doped termination structure**
Qi-Liang Zhang, Shao-Heng Cheng, Liu-An Li and Hong-Dong Li
- 088201 How graph features decipher the soot assisted pigmental energy transport in leaves? A laser-assisted thermal lens study in nanobiophotonics**
S Sankararaman
- 088202 Adaptive semi-empirical model for non-contact atomic force microscopy**
Xi Chen, Jun-Kai Tong and Zhi-Xin Hu
- 088501 Characterization of topological phase of superlattices in superconducting circuits**
Jianfei Chen, Chaohua Wu, Jingtao Fan and Gang Chen
- 088502 Wake-up effect in Hf_{0.4}Zr_{0.6}O₂ ferroelectric thin-film capacitors under a cycling electric field**
Yilin Li, Hui Zhu, Rui Li, Jie Liu, Jinjuan Xiang, Na Xie, Zeng Huang, Zhixuan Fang, Xing Liu and Lixing Zhou
- 088503 A 4×4 metal-semiconductor-metal rectangular deep-ultraviolet detector array of Ga₂O₃ photoconductor with high photo response**
Zeng Liu, Yu-Song Zhi, Mao-Lin Zhang, Li-Li Yang, Shan Li, Zu-Yong Yan, Shao-Hui Zhang, Dao-You Guo, Pei-Gang Li, Yu-Feng Guo and Wei-Hua Tang
- 088701 New insight into the mechanism of DNA polymerase I revealed by single-molecule FRET studies of Klenow fragment**
Rokshana Parvin, Qi Jia, Jianbing Ma, Chunhua Xu, Ying Lu, Fangfu Ye and Ming Li
- 088801 Optical simulation of CsPbI₃/TOPCon tandem solar cells with advanced light management**
Min Yue, Yan Wang, Hui-Li Liang and Zeng-Xia Mei

JUST FOR AUTHORS
— CHINESE PHYSICS B